ACE-FTS measurements across the edge of the winter 2004 Arctic vortex

Ray Nassar,[1] Peter F. Bernath,[1] Chris D. Boone,[1] Gloria L. Manney,[2,3] Sean D. McLeod,[1] Curtis P. Rinsland,[4] Randall Skelton,[1] and Kaley A. Walker[1]

[1]   Atmospheric Chemistry Experiment Fourier Transform Spectrometer (ACE-FTS) solar occultation measurements have been used to create volume mixing ratio (VMR) profiles of H_2O, CH_4, and N_2O inside and outside the 2004 Arctic vortex. Using derived meteorological quantities such as potential vorticity, we have classified 450 occultations (from February and March 2004 spanning 0 to 79.8°N) as vortex, vortex edge, or extravortex. We plot $[CH_4]$ versus $[N_2O]$ correlations to display the distinct patterns observed for measurements of different air masses and use these correlations to further classify the extravortex occultations as tropical, subtropical, or midlatitude. Using comparisons between high latitude profiles of $[N_2O]$, $[CH_4]$, and $[H_2O]$ inside and outside the Arctic vortex, we estimate upper stratospheric and lower mesospheric descent rates and find that descent in the winter 2004 Arctic vortex was rapid, with evidence of descent at higher altitudes than in past years.   **Citation:** Nassar, R., P. F. Bernath, C. D. Boone, G. L. Manney, S. D. McLeod, C. P. Rinsland, R. Skelton, and K. A. Walker (2005), ACE-FTS measurements across the edge of the winter 2004 Arctic vortex, *Geophys. Res. Lett.*, *32*, L15S05, doi:10.1029/ 2005GL022671.

1. Introduction

[2]   In the Brewer-Dobson circulation model, tropical air ascends through the tropical tropopause layer, travels poleward across the stratosphere and mesosphere, then descends at the poles. When a strong polar vortex is present, it can act as a barrier isolating air within it and as a result, vortex air may experience unmixed diabatic cooling and descend. A strong vortex can be identified by a steep gradient in potential vorticity (PV) coincident with the polar-night jet. When the vortex is weak, so is the barrier to transport, and mixing dilutes evidence of descent based on atmospheric tracer species.

[3]   The Arctic vortex is generally warmer, more variable, and more difficult to predict than the Antarctic vortex. Improving our understanding of transport in the Arctic stratosphere is important for understanding Arctic ozone loss. Meteorological analyses indicate that the 2003–2004 Arctic winter was remarkable in the ~50-year record

[*Manney et al.*, 2005]. Overall, stratospheric temperatures were higher than normal and a sudden stratospheric warming starting in late December caused disruptions in the middle and lower stratosphere lasting for weeks to months. However, after a brief disruption in late December/early January, the upper stratospheric vortex redeveloped and was the strongest and coldest on record since February and March 1979 [*Manney et al.*, 2005].

[4]   In this paper, we present ACE-FTS solar occultation measurements, which we classify as vortex, vortex edge, midlatitude, subtropical or tropical, using PV data and $[CH_4]$ versus $[N_2O]$ correlations (where square brackets denote the volume mixing ratio). We then examine profiles of $[N_2O]$, $[H_2O]$, and $[CH_4]$ from the midtroposphere to the mesopause, inside and outside the Arctic polar vortex and use these to estimate descent rates in the vortex.

2. ACE-FTS Retrievals

[5]   The ACE-FTS is the primary instrument on the Atmospheric Chemistry Experiment (ACE) satellite, also known as SCISAT-1. It is a high resolution Fourier transform spectrometer operating in the $750-4400$ cm^{-1} range that measures solar occultation spectra at a series of tangent heights, which are inverted to give profiles of temperature, pressure and molecular VMRs with a vertical resolution of $3-4$ km [*Bernath et al.*, 2005]. Temperature and pressure are retrieved first by fitting measured CO_2 spectral lines to calculated lines from a forward model, then VMR profiles for numerous molecules are retrieved in a similar manner (C. D. Boone et al., Retrievals for the Atmospheric Chemistry Experiment Fourier Transform Spectrometer, submitted to *Applied Optics*, 2005) (hereinafter referred to as Boone et al., submitted manuscript, 2005). ACE-FTS version 1 data include temperature and pressure profiles from the mid-troposphere to the mesopause and VMR profiles of H_2O, N_2O, CO, NO, HCl, HF, HNO_3, CH_4, O_3, NO_2, HDO, SF_6, COF_2, N_2O_5, $ClONO_2$, CCl_3F, CCl_2F_2, and CHF_2Cl on a 1-km grid with statistical uncertainties.

[6]   The H_2O retrieval uses 52 microwindows in the $1362-2137$ cm^{-1} range to retrieve profiles from $7-90$ km altitude. The 64 CH_4 microwindows fall in the $1245-2889$ cm^{-1} range, to retrieve profiles from $4-63$ km altitude. The 62 N_2O microwindows fall in the $1168-2816$ cm^{-1} range to retrieve profiles from $5-60$ km altitude. H_2O and CH_4 each have statistical uncertainties (a measure of the random error in the fitting process that does not include systematic errors) of less than 2% for the strato-

---

[1]Department of Chemistry, University of Waterloo, Waterloo, Ontario, Canada.
[2]New Mexico Highlands University, Las Vegas, New Mexico, USA.
[3]Also at NASA Jet Propulsion Laboratory/California Institute of Technology, Pasadena, California, USA.
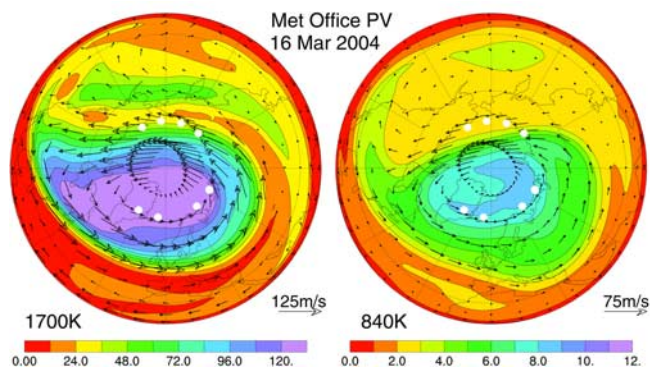[4]NASA Langley Research Center, Hampton, Virginia, USA.

Figure 1. NH potential vorticity (PV) maps for 16 March 2004, 12:00 UT corresponding to θ = 1700 K (~50 km altitude) and θ = 840 K (~30 km). The North Pole is at the center of each map with 90°W at the left and 90°E at the right. The color scale indicates PV (10^{-4} K m^2 kg^{-1} s^{-1}), and the arrows are wind vectors scaled to the arrow at the lower right of the map. The white spots are reference locations for eight occultations measured on 16 March 2004.

sphere but higher in the troposphere and mesosphere. N_2O has statistical uncertainties of less than 2% up to ~38 km, but VMRs above this point are very low so the relative uncertainty is larger. Above the highest measurement for each gas, VMRs are derived by assuming the shape of a climatological a priori profile and multiplying it by a constant determined from the fit (Boone et al., submitted manuscript, 2005).

3. Occultation Classifications

[7] PV maps such as those shown in Figure 1, can be used to check for the presence or location of the polar vortex. We used PV maps based on data from the UK Met Office (MetO), depicting conditions in the upper stratosphere corresponding to an isentropic surface with a potential temperature (θ) of 1700 K (~50 km), the middle stratosphere at θ = 840 K (~30 km) and the lower stratosphere at θ = 465 K (~20 km) at 12:00 UT each day. February and March 2004 PV maps indicated that the northern hemisphere (NH) vortex was strong in the upper stratosphere, highly variable in the middle stratosphere and undefined in the lower stratosphere, so 30–50 km was chosen for determining the location of an occultation with respect to the vortex.

[8] To group profiles resulting from measurements of similar air masses, we developed a system for classifying our occultations that began with determining the location of the vortex edge. For each occultation, θ, PV, and equivalent latitude (EqL, the latitude that would enclose the same area between it and the pole as a given PV contour) were calculated from MetO data, on a 1-km grid from 0.5 to 65.5 km altitude to facilitate use with the ACE-FTS data. The vortex edge was found using a criterion very similar to that described by *Nash et al.* [1996] based on location of maximum PV gradient as a function of EqL, constrained by approximate co-location of maximum wind speed. Since the vortex edge has a finite width, the distance in degrees EqL

from the center of the vortex edge was determined for each tangent point with positive values inside the vortex, negative values outside and null values when no vortex is present. This resulted in an array of EqL-distances which could include positives, negatives and nulls for a single occultation. As with any vortex edge criterion, the best results are obtained when there is a single, strong, unambiguous vortex.

[9] A second set of criteria was established to check the EqL-distance of each tangent point from 30–50 km, to see if it was inside the vortex, outside the vortex or null. If the proportion of tangent points inside minus the proportion outside was greater than 0.5, the occultation was considered inside the vortex and if less than −0.5, it was considered outside. If the difference was greater than or equal to −0.5 and less than or equal to 0.5 and the vortex was present for a significant portion of this range, an occultation was considered on the edge of the vortex. With these criteria we classified all occultations as vortex, extravortex or vortex edge.

[10] Tracer species such as CH_4 and N_2O are useful indicators of the recent dynamical and photochemical history of an air mass. The lifetime of CH_4 is controlled by its rate of oxidation by OH, O(^{1}D), and Cl, whereas the lifetime of N_2O is determined by its rate of UV photolysis or reaction with O(^{1}D) [*Michelsen et al.*, 1998a]. When horizontal mixing is rapid, correlations of these species should be compact, varying only with altitude. Correlations from dynamically isolated air masses may exhibit slight differences that can be used to classify them as tropical, midlatitude or vortex [*Michelsen et al.*, 1998a, 1998b]. Figure 2 is a plot of [CH_4] versus [N_2O] at interpolated tangent points for each of our 450 NH occultations. Using definitions similar to those of *Michelsen et al.* [1998a], we further classified our extravortex occultations as tropical, subtropical and midlatitude. Midlatitude here refers to occultations of any latitude that are both outside the vortex and have no tropical or subtropical characteristics. The dense main group of points is mainly due to midlatitude
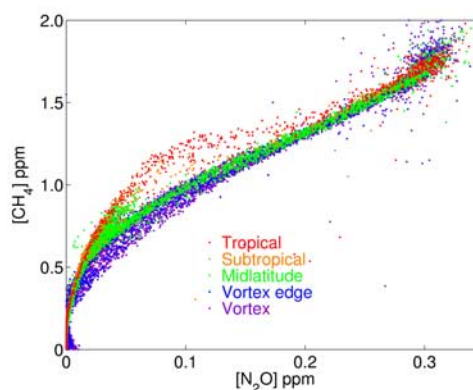

Figure 2. The [N_2O] versus [CH_4] correlation plot for 450 NH occultations during the period of 5 February to 31 March 2004. The color-coded classes (Tropical, Subtropical, Midlatitude, Vortex Edge and Vortex) in the legend loosely correspond to the color scheme for the PV maps in Figure 1.

correlations, with correlations from tropical air above the main line and correlations from within the vortex or vortex edge slightly below and to the right. Subtropical correlations fall between distinct tropical and midlatitude correlations and typically arise from latitudes of $\sim 16-30°N$. There are distinct differences between subtropical, tropical, and midlatitude correlations but the differences between vortex, vortex edge and midlatitude correlations are subtle. The five color-coded classes in Figure 2 loosely correspond to the color scheme on the PV maps. The correspondence is not exact because the vortex edge is defined by a strong PV gradient, rather than a single PV value.

[11] Our classifications are consistent with the upper and middle stratosphere PV maps, as expected, since both utilized the same MetO PV data. However, the accuracy of our classifications is limited by the introduction of derived meteorological products (θ, PV, EqL) from a data assimilation rather than a system based entirely on our own measurements and our use of a single reference location for each occultation. Each occultation is really a series of near-vertical measurements incurring a slight change in latitude, longitude, and time, but this generally has a minor effect on our classifications.

4. Vortex Measurements and Analysis

[12] In February and March 2004, the upper stratospheric Arctic vortex was the strongest since regular observations began in 1979 [*Manney et al.*, 2005]. Figure 1 shows PV maps for 16 March, several days prior to break up, when the center of the vortex was located far off the pole. Figure 3 shows profiles of [N₂O], [H₂O], [CH₄], and potential water (PW), where PW = [H₂O] + 2[CH₄]. PW is a conserved quantity unlike [H₂O] and [CH₄] which fluctuate with the extent of methane oxidation [*Nassar et al.*, 2005]. The eight profiles in Figure 3 were measured on 16 March between $3:48-20:07$ UT, $71.5-72.3°N$ and a range of longitudes, represented by the white spots in Figure 1. The lower four spots (longitudes $64°E$, $40°E$, $33°W$, $58°W$) have been classified as in the vortex and the upper four
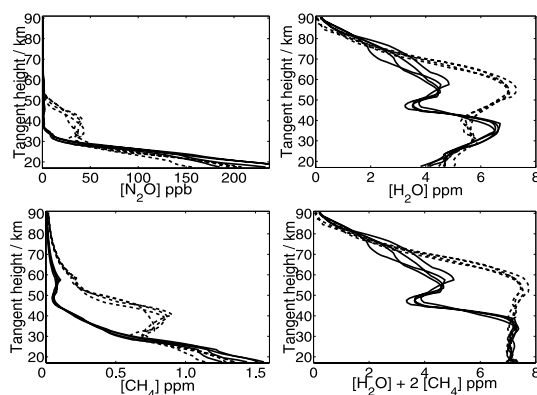

Figure 4. Average [H₂O], [CH₄], [N₂O], and [PW] profiles based on 217 profiles inside the Arctic vortex (solid line) and 47 profiles outside the vortex (dashed line), all measured between 14 February and 22 March 2004 at $60-77°N$. Error bars indicate the variability between profiles.

(longitudes $150°W$, $174°W$, $161°E$, $137°E$) as midlatitude, although they are very close to the dispersed vortex edge. We see clear differences between profiles from inside and outside the vortex even though all were measured within $1°$ of latitude and a time span of less than 17 hours.

[13] *Abrams et al.* [1996a, 1996b] examined differences in ATMOS profiles of [CH₄], [N₂O], and [HF] at midlatitudes and high latitudes both inside and outside the polar vortices. Although they found very little difference between midlatitude and high latitude profiles from outside the vortex, large differences were found between vortex and extravortex profiles. They determined descent rates in the Arctic and Antarctic vortices by dividing the distance separating the profiles by the age of the vortex. The age of the vortex is difficult to define since formation is a gradual process, however, using PV maps we estimate the formation date of the upper stratospheric Arctic vortex as 15 October 2003. Vortex profiles of [N₂O], [CH₄], and [H₂O] near 34 km have VMRs equivalent to extravortex values near 50 km. Assuming unmixed descent (profiles are only altered by vertical motion) during the period of 15 October 2003 to 16 March 2004, we observe 16 km of descent over five months, giving an average descent rate of 3.2 km/month for upper stratospheric air originating in the $40-54$ km range. Since the upper stratospheric vortex broke up and reformed, a value for average descent over the entire winter has little significance. However, by comparing averages of 12 vortex profiles from $18-21$ February at $72.8-75.8°N$ and 10 vortex profiles from $16-20$ March at $65-71.8°N$ (not shown) we obtain 4.5 km of upper stratospheric descent in one month based on CH₄ and H₂O. This is a far better representation of descent during February and March, when the vortex had reformed and strengthened after the late December breakup.

[14] Figure 4 shows averages of 217 [N₂O], [CH₄], [H₂O], and PW profiles classified as inside the polar vortex compared to averages of 47 midlatitude profiles, all measured between 14 February and 22 March at $60-77°N$. The error bars indicate the 1σ variability in the profiles. While changes in the [N₂O] and [CH₄] profiles appear to be

Figure 3. [N₂O], [H₂O], [CH₄], and PW profiles at $\sim 72°N$, inside the Arctic vortex at $64°E$, $40°E$, $33°W$, $58°W$ (solid lines) and outside the Arctic vortex at $150°W$, $174°W$, $161°E$, $137°E$ (dashed lines) on 16 March 2004. The measurement locations are shown in Figure 1.
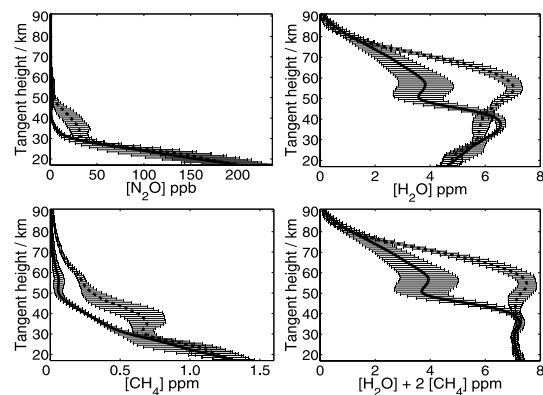
slightly dampened by averaging relative to the 16 March profiles (Figure 3), they are consistent with the results above. All four averaged profile comparisons in Figure 4 also indicate that below ~30 km in altitude, the vortex had a negligible influence. Similarly, the [H_2O] and PW profiles show differences as high as ~77 km, indicating that the vortex may still reduce horizontal mixing at these altitudes. The [H_2O] and PW profiles in Figures 3 and 4 provide good evidence of mesospheric descent; however, the high variability indicated by the error bars in Figure 4 and examination of individual February and March profiles indicate that mixing in the mesosphere had resumed prior to the end of this period, so earlier data was desired to calculate mesospheric descent. [H_2O] and PW for the 12 vortex profiles from February described above, compared with one extravortex profile from 15 February at 63°N (not shown), indicate 21.2 km of descent for air originating in the 60–74 km range. This is an average descent of 5.3 km/month in the lower mesosphere for the period of 15 October 2003 to 15 February 2004. Since mesospheric mixing resumed earlier than in the upper stratosphere, we do not estimate a late winter lower mesospheric descent rate.

5. Discussion and Conclusions

[15] We attribute the differences in vortex and extravortex profiles to dissociation of H_2O, CH_4, and N_2O in the upper stratosphere and mesosphere followed by unmixed descent in the vortex. We attribute the inversions in the [H_2O] and PW profiles near 50 km altitude, which were very pronounced on 16 March but dampened on the average profiles, to the vortex shifting non-uniformly with altitude in the days prior to the final spring break-up.

[16] We have determined an average Arctic vortex descent rate of 3.2 km/month for the upper stratosphere based on N_2O, CH_4, and H_2O and 5.3 km/month for the lower mesosphere based on H_2O and PW. We also calculated an upper stratospheric descent rate of 4.5 km/month based on CH_4 and H_2O, for February and March 2004 when the vortex was strongest. In spite of the temporary disruption to the upper stratospheric vortex, the average stratospheric descent rate is still close to the maximum value observed for the November 1994 Antarctic vortex (3.6 km/month) [*Abrams et al.*, 1996a] and much higher than the maximum for the April 1993 Arctic vortex (2.4 km/month) [*Abrams et al.*, 1996b]. It is also higher than descent rates quoted by *Greenblatt et al.* [2002a, 2002b] which include 11 other studies, although these are all for the middle to lower stratosphere where lower descent rates are expected. Our February-March descent rate is significantly higher than all of these previously measured descent rates. However, *Manney et al.* [1994] modeled descent at a range of altitudes for both hemispheres and obtained a value of 0.3 cm/s equivalent to 7.8 km/month for the 1992–1993 Arctic upper stratospheric vortex at a starting altitude of 47 km. *Rosenfield et al.* [1994] also modeled descent in both hemispheres at a range of altitudes and calculated 27 km of descent for air originating at 50 km. They used 1 November to 21 March as the period of descent, but assuming our descent period yields a rate of 5.4 km/month for the upper stratosphere. *Fisher and O'Neil* [1993]

determined a range of Antarctic vortex descent rates from 3 km/month in the middle stratosphere to 12 km/month in the mesosphere. To our knowledge, the only prior measurements of mesospheric descent were made by *Aellig et al.* [1996] using the Millimeter wave Atmospheric Sounder (MAS) to observe the spring 1992 Arctic vortex, but no estimate of a descent rate was given.

[17] The methods for estimating descent rates presented here are admittedly somewhat crude, yet still give a useful estimate of a difficult-to-measure phenomenon. In the 2003–2004 winter, unmixed descent is a poor assumption since the upper stratospheric vortex completely broke up in late December and recovered in early January [*Manney et al.*, 2005]. While this assumption should not effect our February–March descent rate of 4.5 km/month for the upper stratosphere, the upper stratospheric 2003–2004 winter average descent rate of 3.2 km/month and lower mesospheric average descent rate of 5.3 km/month represent minimum possible values. With limited measurements and no reliable meteorological data for the mesosphere, a more accurate estimate is difficult.

[18] We have shown that PV data and tracer species such as N_2O and CH_4 may be used to classify the type of air mass being measured. We have also demonstrated the strength of the stratospheric vortex as a barrier to horizontal transport by the contrast between profiles of [N_2O], [CH_4], and [H_2O] at similar latitudes inside and outside the vortex, as well as the effective containment of air up into the mesosphere. This work indicates that descent in the winter 2004 Arctic vortex was relatively rapid and that evidence of unmixed descent extended to higher altitudes than observed in past years, likely due to a stronger and more persistent than usual upper stratospheric vortex in late winter.

References

Abrams, M. C., et al. (1996a), Trace gas transport in the Arctic Vortex inferred from ATMOS ATLAS-2 observations during April 1993, *Geophys. Res. Lett.*, *23*(17), 2341–2344.

Abrams, M. C., et al. (1996b), ATMOS/ATLAS-3 observations of long-lived tracers and descent in the Antarctic vortex in November 1994, *Geophys. Res. Lett.*, *23*(17), 2345–2348.

Aellig, C. P., et al. (1996), Space-borne H_2O observations in the Arctic stratosphere and mesosphere in the spring of 1992, *Geophys. Res. Lett.*, *23*(17), 2325–2328.

Bernath, P. F., et al. (2005), Atmospheric Chemistry Experiment (ACE): Mission overview, *Geophys. Res. Lett.*, doi:10.1029/2005GL022386, in press.

Fisher, M., and A. O'Neil (1993), Rapid descent of mesospheric air into the stratospheric polar vortex, *Geophys. Res. Lett.*, *20*(12), 1267–1270.

Greenblatt, J. B., et al. (2002a), Tracer-based determination of vortex descent in the 1999/2000 Arctic winter, *J. Geophys. Res.*, *107*(D20), 8279, doi:10.1029/2001JD000937.

Greenblatt, J. B., et al. (2002b), Correction to "Tracer-based determination of vortex descent in the 1999/2000 Arctic winter" by J. B. Greenblatt et al., *J. Geophys. Res.*, *108*(D5), 8307, doi:10.1029/2002JD001597.

Manney, G. L., et al. (1994), On the motion of air through the stratospheric polar vortex, *J. Atmos. Sci.*, *51*, 2973–2994.

Manney, G. L., K. Krüger, J. L. Sabutis, S. A. Sena, and S. Pawson (2005), The remarkable 2003–2004 winter and other recent warm winters in the Arctic stratosphere since the late 1990s, *J. Geophys. Res.*, *110*, D04107, doi:10.1029/2004JD005367.

Michelsen, H. A., G. L. Manney, M. R. Gunson, C. P. Rinsland, and R. Zander (1998a), Correlations of stratospheric abundances of CH_4 and N_2O derived from ATMOS measurements, *Geophys. Res. Lett.*, *25*(15), 2777–2780.

Michelsen, H. A., G. L. Manney, M. R. Gunson, and R. Zander (1998b), Correlations of stratospheric abundances of NO_y, O_3, N_2O, and CH_4 derived from ATMOS measurements, *J. Geophys. Res.*, *103*(D21), 28,347–28,359.

Nash, E. R., P. A. Newman, J. E. Rosenfield, and M. R. Schoeberl (1996), An objective determination of the polar vortex using Ertel's potential vorticity, *J. Geophys. Res.*, *101*(D5), 9471–9478.

Nassar, R., P. F. Bernath, C. D. Boone, G. L. Manney, S. D. McLeod, C. P. Rinsland, R. Skelton, and K. A. Walker (2005), Stratospheric abundances of water and methane based on ACE-FTS measurements, *Geophys. Res. Lett.*, *32*, L15S04, doi:10.1029/2003GL022383.

Rosenfield, J. E., P. A. Newman, and M. R. Schoeberl (1994), Computations of diabatic descent in the stratospheric polar vortex, *J. Geophys. Res.*, *99*(D8), 16,677–16,689.

—————————————

P. F. Bernath, C. D. Boone, S. D. McLeod, R. Nassar, R. Skelton, and K. A. Walker, Department of Chemistry, University of Waterloo, Waterloo, Ontario, Canada, N2L 3G1. (bernath@uwaterloo.ca; cboone@sciborg.uwaterloo.ca; sdmcleod@uwaterloo.ca; ray@acebox.uwaterloo.ca; skelton@brutus.uwaterloo.ca; kwalker@acebox.uwaterloo.ca)

G. L. Manney, New Mexico Highlands University, Las Vegas, NM 37701, USA. (manney@mls.jpl.nasa.gov)

C. P. Rinsland, NASA Langley Research Center, Mail Stop 401A, Hampton, VA 23681-2199, USA. (c.p.rinsland@larc.nasa.gov)